RSC Advances

PAPER

View Article Online
View Journal | View Issue

Cite this: *RSC Adv.*, 2020, **10**, 32043

Neuroprotective constituents from the aerial parts of *Cannabis sativa* L. subsp. *sativa*†

Jia Li,[a] Guan Wang,[ab] Yu Qin,[a] Xue Zhang,[a] Hai-Feng Wang,[a] Hong-Wei Liu,[c] Ling-Juan Zhu *[ab] and Xin-Sheng Yao *[a]

Received 23rd May 2020
Accepted 12th August 2020

DOI: 10.1039/d0ra04565a

rsc.li/rsc-advances

Five new compounds including three new cannabinoids, cannabisativas A–C (**1–3**), two new phenolic acids, (7*Z*,9*Z*)-cannabiphenolic acid A (**4**) and (8*S*,9*Z*)-cannabiphenolic acid B (**5**), together with twelve known compounds (**6–17**), were isolated from the aerial parts of *Cannabis sativa* L. subsp. *sativa*. The structures of **1–5** were established on the basis of extensive 1D, 2D NMR and HRESIMS analysis. The absolute configurations were determined by comparison between their experimental and calculated spectra of electronic circular dichroism (ECD) or the modified Mosher's method. The neuroprotective effects of the compounds **1–17** were evaluated on PC 12 cells. Compounds **12**, **13** and **15** showed potential protective effects against H_2O_2-induced damage.

Introduction

Alzheimer's disease (AD) is a neurodegenerative disease characterized by impairment in progressive cognition and memory. The main pathological changes in the brains of AD patients include plaques from the deposition of amyloid-β (Aβ), neurofibrillary tangles induced by hyperphosphorylation of microtubule-associated protein–Tau protein, and neuronal degeneration or loss.[1–3] The pathological mechanism of AD is too complicated to be clarified. Hypotheses including β-amyloidogenesis,[4] cholinergic dysfunction,[5] tau hyperphosphorylation,[6,7] and oxidative stress[8,9] have been proposed. Among them, oxidative stress injury was demonstrated to be associated with the aggregation of Aβ, the increase in hyperphosphorylation of tau, and neuronal degeneration.[8,9] The present drugs in clinics can alleviate some clinical symptoms, but are unable to prevent the disease from progressing.[10]

Cannabis sativa L. subsp. *sativa* is a member of the genus *Cannabis* of Cannabaceae. The fruits of *C. sativa* are popular food of Bama Yao Autonomous County in Guangxi province, which is well known as "The Village of Longevity" in China. It has been indicated that long term intake of fruits of *C. sativa* benefited for the health and longevity of local people.[11,12] The extracts of *C. sativa* have been demonstrated to have analgesic, antiemetic, and anxiolytic activities.[13–15] A number of chemical constituents, *e.g.*, cannabinoids (CBDs), mono- and sesquiterpenes, steroids, flavonoids, and nitrogenous compounds, were reported from *C. sativa*.[16] Early studies confirmed CBDs possessed anticonvulsant activity, analgesic and neuroprotective effects.[17–19] CBDs produced neuroprotection through activating the receptors-mediated signal transduction pathways.[20] In our previous study, the ethyl acetate extracts from the aerial parts of *C. sativa* were proved to significantly improve the spatial learning and decrease memory impairment of dementia rats.[21] To discover new anti-AD active constitutes from the aerial parts of *C. sativa*, we conducted a deep investigation on the ethyl acetate extracts from the aerial parts of *C. sativa*. As a result, three new cannabinoids, two new phenolic acids, and twelve known compounds were isolated and structurally determined. In addition, compounds **1–17** were *in vitro* evaluated for their neuroprotective activities.

Results and discussion

Chromatographic separation of the EtOAc extracts from the aerial parts of *C. sativa* yielded five new compounds (**1–5**) and twelve known compounds (**6–17**), named Δ^9-*trans*-tetrahydrocannabivarin (**6**),[22] cannabinol (**7**),[23] cannabispirone (**8**),[24] erythrodiol (**9**),[25] oleanolic acid (**10**),[26] maslinic acid (**11**),[27] *p*-hydroxybenzaldehyde (**12**),[28] (*E*)-methyl *p*-hydroxycinnamate (**13**),[29] (*Z*)-methyl *p*-hydroxycinnamate (**14**),[30] ferulic acid (**15**),[31] phylligenol (**16**),[32] and skullcapflavone II (**17**)[33] (Fig. 1).

Cannabisativa A was obtained as yellowish oil. Based on HRESIMS, its molecular formula was determined as $C_{20}H_{28}O_4$ containing 7 degrees of unsaturation. The ^{1}H NMR spectrum

[a]College of Traditional Chinese Materia Medica, Key Laboratory of Structure-Based Drug Design & Discovery of Ministry of Education, Shenyang Pharmaceutical University, Shenyang 110016, China. E-mail: tyaoxs@jnu.edu.cn; zhulingjuanadele@163.com

[b]State Key Laboratory of Biotherapy, Cancer Center, Department of Gastrointestinal Surgery, West China Hospital, Sichuan University, Collaborative Innovation Center for Biotherapy, Chengdu 610041, China

[c]State Key Laboratory of Mycology, Institute of Microbiology, Chinese Academy of Sciences, Beijing 100101, China

† Electronic supplementary information (ESI) available. See DOI: 10.1039/d0ra04565a

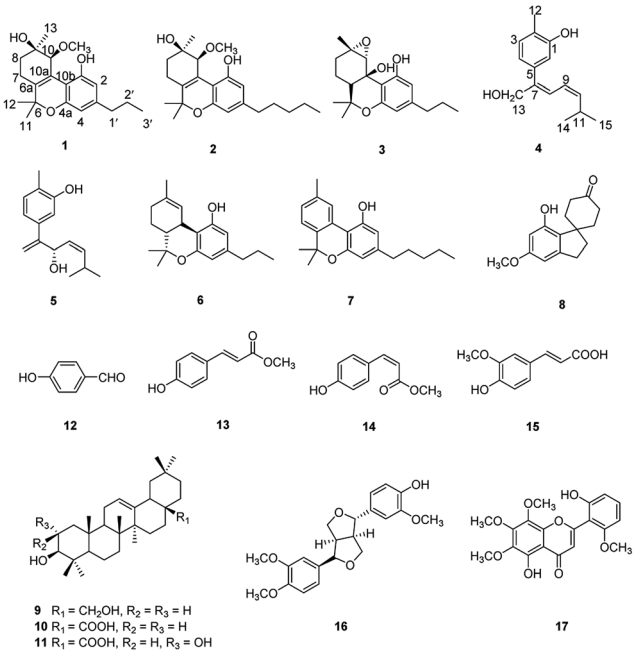

Fig. 1 Structures of the isolated compounds **1–17**.

(Table 1) showed a phenolic hydroxyl at δ_H 9.40 (1H, br s), *meta*-coupled aromatic protons at δ_H 6.35 and 6.28 (each 1H, d, $J = 1.6$ Hz), a methoxy group at δ_H 3.34 (3H, s) and four methyl groups at δ_H 1.50, 1.41, 1.30 and 0.93. ^{13}C NMR and DEPT spectral analyses revealed the presence of eight aromatic/olefinic carbons, two sp^3 quaternary carbons, one sp^3 methine, four sp^3 methylenes, four methyls and one methoxy (Table 1). The ^{1}H and ^{13}C NMR spectra of **1** were quite similar with those of cannabitriol-C_3 (NMR data see Table 1), except that one additional methoxyl at δ_C 51.9 was present in **1**. It was further confirmed by the 2D NMR experiments. The ^{1}H–^{1}H COSY correlations from H-2′ to H-1′ and H-3′, and from H-7 to H-8 confirmed the substructures of $C_{1'}$–$C_{2'}$–$C_{3'}$ and C_7–C_8 (Fig. 2). The key HMBC correlations of H-10/C-6a, C-10a, C-10b, C-8; H-7/C-6a; H-13/C-9; H-12/C-4a, C-6, and H-11/C-6a, C-6 permitted the establishment of a cannabitriol structure. The methoxy and the $C_{1'}$–$C_{2'}$–$C_{3'}$ unit was found to be attached to C-10 and C-3 according to HMBC correlation observed between 10-OC<u>H</u>$_3$/C-10 and H-1′/C-3, respectively.

The relative configuration of **1** (9*R**,10*S**) were supported by observed correlation of H-10/H-13 in ROESY spectrum. To determine the absolute configuration, ECD calculation method using time-dependent density functional theory (TDDFT) and metal rhodium salt method were both applied. The experimental ECD spectrum of **1** matched well with the calculated spectrum for the 9*R*,10*S* configuration (Fig. 3). The absolute configuration was also verified by testing CD difference spectrum after the reaction of C-9 hydroxyl group with metal rhodium salt.[34] The CD difference spectrum showed a negative Cotton effect at 350 nm (Fig. 4), suggesting the absolute configuration at C-9 was inferred to be *R*-form. Thus, **1** was identified as (9*R*,10*S*)-9-hydroxy-10-methoxy-$\Delta^{6a(10a)}$-tetrahydrocannabivarin.

Table 1 NMR spectroscopic data of compounds **1-3** and cannabitriol-C_3 (in $CDCl_3$)

	1		**2**		**3**		Cannabitriol-C_3	
No.	δ_H (J in Hz)	δ_C	δ_H (J in Hz)	δ_C	δ_H (J in Hz)	δ_C	δ_H (J in Hz)	δ_C
1		153.4		153.4		155.4		152.2
2	6.35, d (1.6)	111.2	6.36, d (1.6)	111.1	6.17, d (1.4)	109.4	6.34, d (1.6)	110.9
3		144.8		145.1		144.5		144.5
4	6.28, d (1.6)	108.7	6.28, d (1.6)	108.6	5.95, d (1.4)	108.3	6.30, d (1.6)	109.3
4a		153.5		153.5		153.7		153.7
6		76.3		76.3		75.7		76.6
6a		138.1		138.0	1.49, m	46.9		136.1
7	2.20, dd (19.3, 6.2)	22.1	2.20, dd (19.3, 6.0)	22.1	1.35, m	17.1	2.14, dt (19.0, 4.7)	22.6
	2.45, m		2.46, m		1.67, m		2.39, m	
8	1.75, m	30.9	1.75, m	30.9	1.81, ddd (14.5, 13.0, 4.6)	29.7	1.78, m	29.1
	1.89, dd (14.2, 7.3)		1.89, dd (14.2, 7.3)		2.06, dt (14.5, 3.2)			
9		70.1		70.1		61.6		70.5
10	4.27, br s	77.6	4.27, br s	77.6	3.87, s	66.3	4.19, br s	72.4
10a		117.8		117.8		68.7		122.2
10b		108.4		108.3		109.0		109.0
11	1.30, s	23.7	1.30, s	23.7	1.39, s	25.8	1.23, s	23.5
12	1.50, s	25.4	1.50, s	25.4	1.40, s	27.7	1.45, s	25.2
13	1.41, s	26.3	1.41, s	26.3	1.45, s	22.6	1.39, s	25.1
1′	2.45, m	37.7	2.46, m	35.6	2.27, m	37.6	2.45, t (7.2)	37.7
2′	1.60, m	23.8	1.58, m	30.4	1.48, m	23.7	1.60, m	23.9
3′	0.93, t (7.3)	13.9	1.30, m	31.5	0.87, t (7.3)	14.0	0.92, t (7.3)	13.8
4′			1.31, m	22.5				
5′			0.88, t (6.9)	14.0				
1-OH	9.40, br s		9.40, br s		7.38, br s		8.57, br s	
10-OC<u>H</u>$_3$	3.34, s	51.9	3.34, s	51.9				

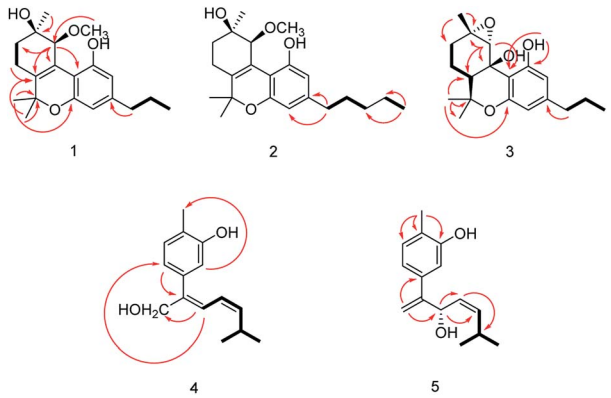

Fig. 2 Key ^{1}H–^{1}H COSY ▬, HMBC ⟶ correlations of compounds **1-5**.

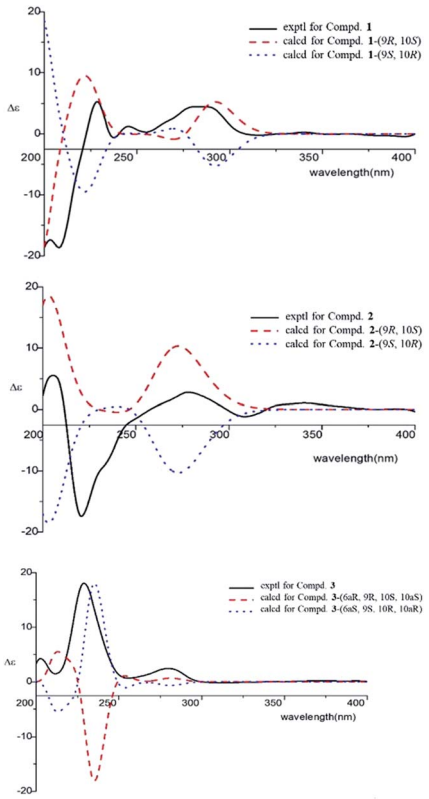

Fig. 3 ECD spectra for compounds **1–3**.

Cannabisativa B was obtained as yellowish oil. The molecular formula of $C_{22}H_{32}O_4$ was assigned on the basis of HRESIMS ion peak at *m*/*z* 361.2383 $[M + H]^+$, requiring 7 degrees of unsaturation. Comparisons of the ^{1}H NMR and ^{13}C NMR spectroscopic data of **2** with those of **1**, additional δ_H 1.30 (2H, m), 1.31 (2H, m); δ_C 30.4, 31.5 were observed in **2**. These signals were positioned at C-3 based on the ^{1}H–^{1}H COSY (H-5′/H-4′; H-2′/H-3′, H-1′) and HMBC (H-5′/C-3′, C-4′; H-1′/C-3, C-4) correlations (Fig. 2). The configuration of **2** was determined as 9*R*,10*S* using the same method of **1** (Fig. 3). Accordingly, **2** was established as (9*R*,10*S*)-9-hydroxy-10-methoxy-$\Delta^{6a(10a)}$-tetrahydrocannabinol.

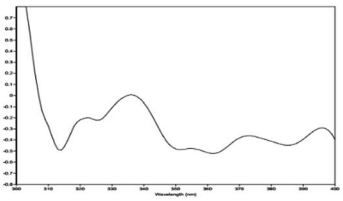

Fig. 4 The CD difference spectrum of $Rh_2(OCOCF_3)_4$ bind with compound **1**.

Cannabisativa C was obtained as yellowish oil, and showed an HRESIMS peak at *m*/*z* 317.1758 $[M–H]^-$, indicating a molecular formula of $C_{19}H_{26}O_4$ and 7 degrees of unsaturation. The ^{1}H NMR spectrum (Table 1) of **3** showed two *meta*-coupled aromatic protons (δ_H 6.17, 5.95 (each 1H, d, $J = 1.4$ Hz)), two sp^3 methine protons (δ_H 1.49, 3.87), four sets of methylenes and four methyls (δ_H 1.39, 1.40, 1.45 and 0.87). The ^{1}H–^{1}H COSY correlations from H-2′ to H-1′ and H-3′, and from H-7 to H-8 and H-6a confirmed the substructures of $C_{1'}$–$C_{2'}$–$C_{3'}$ and C_{6a}–C_7–C_8 (Fig. 2). The key HMBC correlations of 1-OH/C-1, C-10b; H-10/C-6a, C-9, C-10a, C-10b; H-11/C-4a, C-6, C-6a, C-12; H-12/C-4a, C-6, C-6a, C-11; H-13/C-8, C-9, C-10 permitted the establishment of a cannabitriol structure. The $C_{1'}$–$C_{2'}$–$C_{3'}$ unit was found to be attached to C-3 according to HMBC correlation observed between H-1′/C-3. In addition, the chemical shifts of C-9 and C-10 and the molecular formula of **3** indicated the presence of an oxirane ring between C-9 and C-10.

The relative configuration was established by NOESY experiment. Correlations of H-13/H-10, H-7b; H-7b/OH-10a suggested that they were situated in the axial position. Correlation of H-6a/H-8a suggested that they were in the equatorial position. Moreover, the calculated ECD spectrum of (6a*S*,9*S*,10*R*,10a*R*) were matched well with the experimental ECD spectrum of **3** (Fig. 3). Therefore, the structure of **3** was defined as (6a*S*,9*S*,10*R*,10a*R*)-9,10-epoxy-10a-hydroxy-tetrahydrocannabivarin.

Compound **4** was obtained as yellowish oil and had a molecular formula of $C_{15}H_{20}O_2$ as judged from HRESIMS *m*/*z* 231.1380 $[M–H]^-$ (calcd. for $C_{15}H_{19}O_2$ 231.1385), indicative of 6 degrees of unsaturation. The ^{13}C NMR (Table 2) showed three methyls, one methlene, seven methines and four quaternary carbons. In the ^{1}H NMR spectrum, the characteristic signals indicated a 1,3,4-trisubstituted benzene ring at δ_H 7.11 (1H, d, $J = 7.7$ Hz), 6.76 (1H, br d, $J = 7.7$ Hz), 6.71 (1H, br s), two double bonds at δ_H 6.58 (1H, d, $J = 11.5$ Hz), 5.95 (1H, dd, J = 11.5, 11.2 Hz), 5.28 (1H, dd, J = 11.2, 10.3 Hz), a hydroxymethyl group at δ_H 4.40 (2H, m) and three methyl groups at δ_H 2.25 (3H, s), 1.00 (3H, d, $J = 6.6$ Hz) and 0.99 (3H, d, $J = 6.6$ Hz). The ^{1}H–^{1}H COSY correlations of H-11/H-10/H-14 (H-15), and H-9/H-8/H-10 combined with HSQC confirmed the C_8–C_9–C_{10}–C_{11}–C_{14}(C_{15}) moiety (Fig. 2). HMBC correlations fromH-4 to C-7, H-12 to C-1, 2 and 3, and H-13 to C-5 and C-8 (Fig. 2) confirmed the planar structure. The geometry of Δ^7 double bond was determined by NOE difference spectra. Irradiation of H-13 resonance did not lead to a marked enhancement of the H-8 proton signal, and irradiation of the

Table 2 NMR spectroscopic data of compounds **4–5** (in $CDCl_3$)

	4		**5**	
No.	δ_H (J in Hz)	δ_C	δ_H (J in Hz)	δ_C
1		153.7		153.9
2		123.1		123.7
3	7.11, d (7.7)	131.0	7.04, d (7.6)	130.8
4	6.76, br d (7.7)	121.3	6.85, br d (7.6)	119.2
5		137.0		138.5
6	6.71, br s	115.5	6.87, br s	113.8
7		140.5		150.4
8	6.58, d (11.5)	122.4	5.36, overlap	69.9
9	5.95, dd (11.5, 11.2)	122.6	5.31, overlap	127.7
10	5.28, dd (11.2, 10.3)	141.6	5.29, overlap	140.6
11	2.88, m	27.0	2.62, br s	27.2
12	2.25, s	15.5	2.21, s	15.6
13	4.40, s	67.9	5.34, overlap 5.26, br s	112.9
14	1.00, d (6.6)	23.1	0.97, d (6.6)	23.2
15	0.99, d (6.6)	23.1	0.79, d (6.6)	22.6

H-8 also did not cause an enhancement of the H-13. Next, we used ^{13}C NMR calculation as well as DP4+ probability analyses to determine the geometry of Δ^7 double bond. The ^{13}C NMR chemical shifts of **4a** and **4b** were calculated at the B3LYP/6-311 + G(d,p) level utilizing the polarizable continuum model (PCM) in methanol. The calculated results for **4b** ($R^2 = 0.9987$) were a better match with the experimental data than those of **4a** ($R^2 = 0.9951$) (Fig. 5). Moreover, according to the DP4+ probability analyses, **4b** was assigned with a 100% probability (Fig. S41†). Finally, the structure of compound **4** was identified and named as (7*Z*,9*Z*)-cannabiphenolic acid A.

Compound **5**, obtained as yellowish oil, displayed an HRESIMS peak at *m*/*z* 231.1387 $[M–H]^-$ corresponding to the molecular formula $C_{15}H_{20}O_2$, suggesting 6 degrees of unsaturation. Its ^{13}C NMR and DEPT spectra (Table 2) displayed 15 carbon resonances, including three methyls, one methlene, seven methines and four quaternary carbons. The ^1H NMR spectrum showed an 1,3,4-trisubstituted benzene ring at δ_H 7.04 (1H, d, $J = 7.6$ Hz), 6.87 (1H, br s), 6.85 (1H, br d, $J = 7.6$ Hz), a double bond at δ_H 5.31 (1H, overlap) and 5.29 (1H, overlap), a terminal double

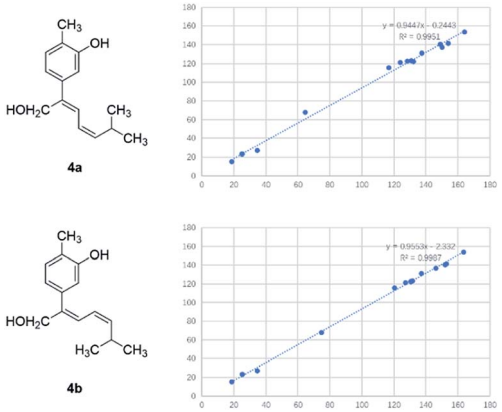

Fig. 5 ^{13}C NMR calculation results of two possible isomers of **4**.

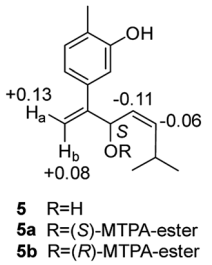

5 R=H
5a R=(*S*)-MTPA-ester
5b R=(*R*)-MTPA-ester

Fig. 6 $\Delta\delta$ ($\delta_{5a} - \delta_{5b}$ in ppm) obtained for the MTPA esters of compound **5**.

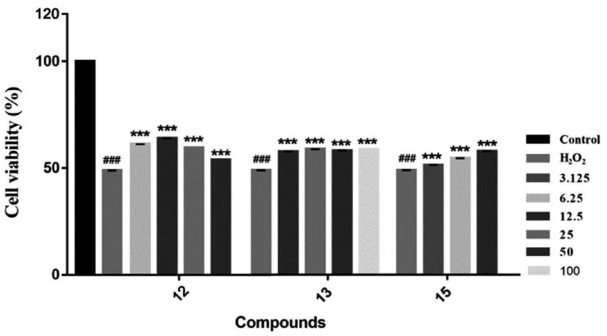

Fig. 7 Neuroprotective effects of compounds against H_2O_2-induced cell growth inhibition of PC12 cells. In the presence or absence of the tested compounds at different concentrations, MTT assay was used to examine the cell viability after H_2O_2 (200 μM) treatment for 4 h $^{***}P <$ 0.001 *vs.* H_2O_2-treated group; $^{\#\#\#}P < 0.001$ was considered statistically significant when compared with its enantiomer.

bond at δ_H 5.34 (1H, overlap) and 5.26 (1H, br s), and three methyl groups at δ_H 2.21 (3H, s), 0.97 (3H, d, $J = 6.6$ Hz) and 0.79 (3H, d, $J = 6.6$ Hz). The C_{10}–C_{11}–C_{14}(C_{15}) moiety was verified by the ^1H–^1H COSY correlations of H-11/H-10/H-14/H-15 (Fig. 2). The key HMBC (Fig. 2) correlations from H-8 to C-9, and C-10, H-9 to C-11, H-12 to C-1, C-2, and C-3, and H-13 to C-5, and C-8 connected the planar structure of compound **5**. The geometry of Δ^9 was assigned as *Z* by the coupling constant ($J_{9,10} = 8.6$ Hz) in pyridine-d_5 (400 MHz). The absolute configuration of C-8 was identified by a modified Mosher's method (Fig. 6). Compound **5** was treated separately with (*R*)- and (*S*)-MTPA-Cl to obtained the respective (*S*)- and (*R*)-MTPA esters (**5a** and **5b**). The *S* configuration of C-8 was determined by the $\Delta\delta_{H(S-R)}$ value of H-9, H-10, H-13a and H-13b. Based on the above findings, compound **5** was named as (8*S*,9*Z*)-cannabiphenolic acid B.

We evaluated the cytotoxicity of compounds **1–17** against PC12 cells using MTT method. Neuroprotective assays were performed at concentrations that had no significant effect on cell survival (compounds **1–5**, **7**, **8** and **12–16**, cell survival rate > 90%) (Table S1†). We found that the novel compounds **1–5** can slightly improve the cell viability, but the significant difference is not obvious. Known compounds **12**, **13** and **15** could attenuate H_2O_2-induced cytotoxicity in PC12 cells by the effect of antioxidant (Fig. 7).

Conclusions

In summary, three new cannabinoids, cannabisativas A–C (**1–3**), two new phenolic acids, (7*Z*,9*Z*)-cannabiphenolic acid A (**4**) and (8*S*,9*Z*)-cannabiphenolic acid B (**5**), along with twelve known compounds (**6–17**), were identified from the aerial parts of *Cannabis sativa* L. subsp. *sativa*. All of the compounds were screened for their neuroprotective activity. The results indicated that compounds **1–5**, can slightly improve the cell viability and **12**, **13** and **15** showed potential protective effects against H_2O_2-induced damage.

Experimental section

General experimental procedures

UV spectra were recorded on a Shimadzu UV-1700 PharmaSpec UV-visible spectrophotometer. The ^{1}H, ^{13}C, and 2D nuclear magnetic resonance (NMR) spectra were measured by a Bruker AVANCE-600 NMR spectrometer (Rheinstetten, Germany) with tetramethylsilane (TMS) as an internal standard. HRESIMS data were acquired using a Waters Synapt G2 QTOF mass spectrometer (Milford, CT, USA). ECD spectra were taken on a Biologic MOS-450. Optical rotations were measured using a JASCO VP-1020.

For column chromatography (CC), silica gel (100–200 and 200–300 mesh, Qingdao, China), Sephadex LH-20 (Uppsala, Sweden) and ODS (60–80 μm, Tokyo, Japan) was used. The analytical HPLC was obtained with an Agilent 1200 (CA, USA) with a DAD detector using a reversed-phase C18 column (5 μm, 250 × 4.60 mm). Semi-preparative HPLC was performed on a Shimadzu LC-6AD (Kyoto, Japan) equipped with a UV SPD-20A detector using a reversed-phase C18 column (5 μm, 250 × 10 mm).

Plant materal

The *Cannabis sativa* L. subsp. *sativa* were collected from Bama Yao Autonomous County, Guangxi Province, China, in December 2014, and identified by Professor Liying Yu (Guangxi Botanical Garden of Medicinal Plants, Guangxi, China). A voucher specimen (YWGCS-2014) was deposited at the School of Traditional Chinese Materia Medica, Shenyang Pharmaceutical University, China.

Extraction and isolation

The dried aerial parts of *C. sativa* (20 kg) were extracted with 70% EtOH (200 L × 2) for 2 h to afford a crude extract (449.2 g), which was suspended in H_2O (5 L) and then partitioned with EtOAc (5 L × 3) and *n*-BuOH (5 L × 3). The EtOAc soluble extract (121.4 g) was subjected to CC over silica gel eluted with cyclohexane/EtOAc (from 100 : 0 to 0 : 100) to afford Fr. EA–EL.

Fr. EC (3.2 g) was subjected to fractionation on ODS column using a stepwise gradient of MeOH–H_2O to give Fr. EC1–EC7. Fr. EC2 (245.1 mg) was further purified by preparative TLC (cyclohexane–EtOAc, 8 : 2) and semi-preparative HPLC using 60% MeOH to afford compound **1** (6.6 mg) and 2 (3.5 mg). Fr. EC4 (723.2 mg) was purified by semi-preparative HPLC (71% MeOH) to yield compound **3** (12.8 mg) and **6** (189.0 mg). Compound **7** (57.2 mg) was afforded from Fr. EC5 (67.5 mg) by purification with semi-preparative HPLC (80% MeOH). Fr. EG (2.4 g) was loaded onto a Sephadex LH-20 column to yield Fr. EG1–EG3. Fr. EG2 (483.3 mg) was subjected to ODS column eluted with the gradient solvent system of MeOH/H_2O, and Fr. EG25 (123.8 mg, 90%MeOH) was purified using semi-preparative HPLC (80% MeOH) to furnish compound **9** (23.7 mg). Fr. EG3 (1.2 g) was divided into two subfractions by ODS gel CC eluted with MeOH/H_2O (from 30% to 50%). Fr. EG31 (62.8 mg) was subjected to purification by a semi-preparative HPLC using 25% MeOH–H_2O to afford compound **12** (31.8 mg). Fr. EG32 (857.2 mg) was subjected to purification by a semi-preparative HPLC using 50% MeOH to afford compound **13** (641.0 mg) and compound **14** (11.8 mg). Fr. EH (2.7 g) was fractioned on CC of Sephadex LH-20 (CH_2Cl_2–MeOH, 1 : 1) to give Fr. EH1–EH3. Fr. EH2 (1.3 g) further separated to five fractions by CC of silica gel. Fr. EH22 (1.0 g, eluted with cyclohexane–EtOAc, 9 : 1) was subjected to ODS CC using 90% MeOH and then purified by semi-preparative HPLC (80% MeOH) to give compound **10** (32.1 mg). Fr. EH3 (506.6 mg) was purified by ODS CC, then Fr. EH323 (109.0 mg, eluted with 50% MeOH) was purified by semi-preparative HPLC (57% MeOH) to give compound **8** (81.2 mg). Fr. EH324 (108.4 mg, eluted with 60% MeOH) was purified by semi-preparative HPLC (55% MeOH) to give compound **5** (5.6 mg). Fr. EI (5.8 g) was applied to a Sephadex LH-20 column using CH_2Cl_2–MeOH (1 : 1) as the eluent to gain two subfractions. Fr. EI2 (4.7 g) was fractionated over silica gel CC to give five subfractions. Fr. EI23 (1.0 g, eluted with cyclohexane–EtOAc, 8 : 2) was further subjected to an ODS column and separated by semi-preparative HPLC (35% MeOH) to afford compound **4** (5.6 mg). Fr. EI24 (2.5 g, eluted with cyclohexane–EtOAc, 7 : 3) was further subjected to an ODS column and separated by semi-preparative HPLC (70% MeOH) to afford compound **17** (110.8 mg). Fr. EK (4.5 g) was subjected to fractionation on Sephadex LH-20 column to yield Fr. EK1–EK3. Fr. EK2 (2.3 g) was fractionated over silica gel CC to give seven subfractions. Fr. EK25 (1.0 g eluted with cyclohexane–EtOAc, 7 : 3) was subjected to ODS CC. Fr. EK253 (392.8 mg, 40% MeOH) was purified by semi-preparative HPLC (42% MeOH) to give compound **16** (218.3 mg). Fr. EK256 (174.7 mg, 50% MeOH) was purified by semi-preparative HPLC (70% MeOH) to give compound **11** (36.1 mg). Fr. EK3 (3.2 g) was fractionated over silica gel CC and further separated by ODS CC and purified by semi-preparative HPLC (20% MeOH) to give compound 15 (92.9 mg).

Cannabisativa A (1). Yellowish oil; $[\alpha]_D^{20}$ −21.0 (*c* 1.0, MeOH); UV (MeOH) λ_{max} (log ε): 228 (3.47) nm, 279 (3.18) nm; ^{1}H and ^{13}C NMR data see Table 1; HRESIMS *m*/*z* 333.2071 $[M + H]^+$ (calcd 333.2066, $C_{20}H_{29}O_4$).

Cannabisativa B (2). Yellowish oil; $[\alpha]_D^{20}$ −23.0 (*c* 1.0, MeOH); UV (MeOH) λ_{max} (log ε): 228 (3.43) nm, 279 (3.10) nm; ^{1}H and ^{13}C NMR data see Table 1; HRESIMS *m*/*z* 361.2383 $[M + H]^+$ (calcd 361.2379, $C_{22}H_{33}O_4$).

Cannabisativa C (3). Yellowish oil; $[\alpha]_D^{20}$ +35.0 (*c* 1.0, MeOH); UV (MeOH) λ_{max} (log ε): 230 (3.33) nm, 282 (3.80) nm; ^{1}H and

^{13}C NMR data see Table 1; HRESIMS *m*/*z* 317.1758 [M–H]$^-$ (calcd 317.1753, $C_{19}H_{25}O_4$).

(7*Z*,9*Z*)-Cannabiphenolic acid A (4). Yellowish oil; UV (MeOH) λ_{max} (log ε): 247 (2.92) nm, 284 (2.62) nm; ^{1}H and ^{13}C NMR data see Table 2; HRESIMS *m*/*z* 231.1380 [M–H]$^-$ (calcd 231.1385, $C_{15}H_{19}O_2$).

(8*S*,9*Z*)-Cannabiphenolic acid B (5). Yellowish oil; UV (MeOH) λ_{max} (log ε): 226 (3.14) nm, 275 (2.99) nm; ^{1}H and ^{13}C NMR data see Table 2; HRESIMS *m*/*z* 231.1387 [M–H]$^-$ (calcd 231.1385, $C_{15}H_{19}O_2$).

ECD calculations

The absolute configurations of compounds **1–3** were determined by using time-dependent density functional theory (TDDFT) calculations carried out with the Gaussian 09 package. First, they were built in GaussianView and subjected to systematic conformational search by CONFLEX. Conformations whose energy was within 3 kcal mol^{-1} from the conformation with the lowest energy were selected for subsequent calculations. Next, the geometries of the compounds were optimized at the B3LYP/6-31G (d) level and the ECD of the conformers was calculated at the B3LYP/6-311++G (2d, p) level with the CPCM solvation model, where MeOH was used as the solvent to match the experimental conditions. The calculated ECD curve was generated using SpecDis 1.51 and compared with the experimental ECD curve to determine their absolute configurations.

Metal rhodium salt method

1.0 mg of compound **1** was dissolved in a dry solution of the stock $[Rh_2(OCOCF_3)_4]$ complex (6.0 mg) in CH_2Cl_2 (200 mL) and tested its CD spectrum immediately, then obtained the CD spectrum of Compd-Rh-CD1. After the reaction, the CD spectrum was tested again, and the CD spectrum of Compd-Rh-CD2 was obtained. After subtracting Compd-Rh-CD1 from Compd-Rh-CD2, we got the CD difference spectrum, and observed the Cotton effect at 350 nm.

NMR calculations

The plausible conformers of compounds **4a** and **4b** were performed by Gaussian 09 software. All obtained conformers were subsequently optimized at the B3LYP/6-31+G(d) level in a methanol solvent model.[35] The Boltzmann-weighted conformer population was calculated by the Gibbs free energy from the geometry optimization step. Then, Boltzmann-weighted averages of the chemical shifts were calculated to scale them against the experimental values. The DP4+ probability was applied to compute the chemical shift errors.

Modified Mosher's method

Compound **5** (0.5 mg) was reacted with *R*-MTPA-Cl (10 μL) in pyridine (0.5 mL) under the protection of nitrogen. The mixture was heated at 50 °C for 4 hours to obtain *S*-MTPA ester. Using the same procedure as described above to obtain the *R*-MTPA ester. ^{1}H-NMR was used to analyze the absolute configuration of the compound.

***S*-MTPA ester of 5.** ^{1}H NMR (400 MHz, pyridine-d_5) δ 5.58 (br s H-13), 5.55 (br s, H-13), 5.49 (overlap, H-10), 5.40 (overlap, H-9).

***R*-MTPA ester of 5.** ^{1}H NMR (400 MHz, pyridine-d_5) δ 5.55 (overlap, H-10), 5.51 (overlap, H-9), 5.47 (br s, H-13), 5.45 (br s, H-13).

Cell culture

PC 12 cells (ATCC, Manassas, VA, USA) were cultured on RPMI-1640 (Roswell Park Memorial Institute) medium with 10% fetal bovine serum, 2 mM l-glutamine, 100 units per mL penicillin and 0.1 mg mL^{-1} streptomycin in a humidified incubator at 37 °C and in 5% CO_2.

Neuroprotective activity assay

The PC12 cells were seeded in 96-well plates at a density of 1×10^5 cells per mL in 90 μL of medium for 24 h. Then treated with different concentrations of compounds or H_2O_2 (200 μM) for 24 h. Cell viability was estimated by MTT colorimetric assay. 10 μL of MTT (5 mg mL^{-1}) was added to each well for 4 h culture. Subsequently, the medium was removed and the formazan crystals were dissolved by dimethyl sulfoxide. The absorbance of formazan solution was measured at 490 nm (Bio-Rad Model 680, Bio-Rad, Hercules, CA, USA).

Conflicts of interest

The authors declare no competing financial interest.

Acknowledgements

This work was supported by the National Natural Science Foundation of China (Grant No. 31970374) and the China Postdoctoral Science Foundation (Grant No. 2016M602697, No. 2018T110988).

References

1 M. Goedert and M. G. Spillantini, *Science*, 2006, **314**, 777–781.
2 S. D. Skaper, *Int. Rev. Neurobiol.*, 2012, **102**, 277–316.
3 P. H. Reddy, M. Manczak, P. Mao, M. J. Calkins, A. P. Reddy and U. Shirendeb, *J. Alzheimer's Dis.*, 2010, **20**, S499–S512.
4 J. Apelt, M. Bigl, P. Wunderlich and R. Schliebs, *Int. J. Dev. Neurosci.*, 2004, **22**, 475–484.
5 A. Bellucci, I. Luccarini, C. Scali, C. Prosperi, M. G. Giovannini, G. Pepeu and F. Casamenti, *Neurobiol. Dis.*, 2006, **23**, 260–272.
6 G. Amadoro, V. Corsetti, M. T. Ciotti, F. Florenzano, S. Capsoni, G. Amato and P. Calissano, *Neurobiol. Aging*, 2011, **32**, 969–990.
7 L. M. Ittner and J. Götz, *Nat. Rev. Neurosci.*, 2011, **12**, 67–72.
8 H. Lee, G. Perry, P. I. Moreira, M. R. Garrett, Q. Liu, X. Zhu, A. Takeda, A. Nunomura and M. A. Smith, *Trends Mol. Med.*, 2005, **11**, 164–169.

9 Z. Tucsek, P. Toth, D. Sosnowska, T. Gautam, M. Mitschelen, A. Koller, G. Szalai, W. E. Sonntag, Z. Ungvari and A. Csiszar, *J. Gerontol., Ser. A*, 2013, **69**, 1212–1226.
10 J. O. Fajemiroye, *Med. Chem.*, 2014, **4**, 697–703.
11 A. Smeriglio, S. V. Giofrè, E. M. Galati, M. T. Monforte, N. Cicero, V. D'Angelo, G. Grassi and C. Circosta, *Fitoterapia*, 2018, **127**, 101–108.
12 H. B. Li, S. H. Wu, Y. Y. Zhang, Y. J. Qi, N. Lv, G. L. Li and J. Z. Ma, *Chin. Tradit. Herb. Drugs*, 2018, **49**, 3334–3342.
13 J. D. Roberts, C. Gennings and M. Shih, *Eur. J. Pharmacol.*, 2006, **530**, 54–58.
14 N. A. Darmani and J. C. Johnson, *Eur. J. Pharmacol.*, 2004, **488**, 201–212.
15 E. Murillo-Rodríguez, D. Millán-Aldaco, M. Palomero-Rivero, R. Mechoulam and R. Drucker-Colín, *FEBS Lett.*, 2006, **580**, 4337–4345.
16 S. A. Ahmed, S. A. Ross, D. Slade, M. M. Radwan, F. Zulfiqar and M. A. ElSohly, *J. Nat. Prod.*, 2008, **71**, 536–542.
17 N. A. Jones, A. J. Hill, I. Smith, S. A. Bevan, C. M. Williams, B. J. Whalley and G. J. Stephens, *J. Pharmacol. Exp. Ther.*, 2010, **332**, 569–577.
18 B. Costa, A. E. Trovato, F. Comelli, G. Giagnoni and M. Colleoni, *Eur. J. Pharmacol.*, 2007, **556**, 75–83.
19 A. Ligresti, L. D. Petrocellis and V. D. Marzo, *Physiol. Rev.*, 2016, **96**, 1593–1659.
20 H. Li, Y. Z. Liu, D. N. Tian, L. Tian, X. K. Ju, L. Qi, Y. B. Wang and C. Y. Liang, *Eur. J. Med. Chem.*, 2020, **192**, 112163.
21 G. Wang, L. J. Zhu, Y. Q. Zhao, S. Y. Gao, D. J. Sun, J. Q. Yuan, Y. X. Huang, X. Zhang and X. S. Yao, *Bioorg. Chem.*, 2017, **72**, 64–73.
22 A. Hazekamp, A. Peltenburg, R. Verpoorte and C. Giroud, *J. Liq. Chromatogr. Relat. Technol.*, 2005, **28**, 2361–2382.
23 Y. H. Choi, A. Hazekamp, A. M. G. Peltenburg-Looman, M. Frédérich, C. Erkelens, A. W. M. Lefeber and R. Verpoorte, *Phytochem. Anal.*, 2004, **15**, 345–354.
24 M. M. Radwan, S. A. Ross, D. Slade, S. A. Ahmed, F. Zulfiqar and M. A. ElSohly, *Planta Med.*, 2008, **74**, 267–272.
25 H. Takahashi, M. Iuchi, Y. Fujita, H. Minami and Y. Fukuyama, *Phytochemistry*, 1999, **51**, 543–550.
26 S. J. Shin, C. E. Park, N. I. Baek, I. S. Chung and C. H. Park, *Biotechnol. Bioprocess Eng.*, 2009, **14**, 140–145.
27 W. J. He, F. li, C. Y. Yang and M. K. Wang, *Chin. J. Appl. Environ. Biol.*, 2014, **20**, 846–849.
28 N. Bouaicha, P. Amade, D. Fuel and C. Roussakis, *J. Nat. Prod.*, 1994, **57**, 1455–1457.
29 Y. Hiraga, L. Chen, M. Kurokawa, S. Ohta, T. Suga and T. Hirata, *Nat. Prod. Lett.*, 1996, **9**, 21–26.
30 Q. Cheng, Y. W. Zhang, X. Zhang and T. Oritani, *Chin. Chem. Lett.*, 2003, **14**, 1215–1218.
31 W. J. Xiang and J. S. Wen, *J. Anhui Agric. Sci.*, 2012, **40**, 2651–2653.
32 S. K. R. Morais, A. F. Teixeira, Z. E. D. S. Torres, S. M. Nunomura, E. H. Yamashiro-Kanashiro, J. A. L. Lindoso and M. Yoshida, *J. Braz. Chem. Soc.*, 2009, **20**, 1110–1118.
33 W. Li, X. Pang, L. F. Han, Y. Zhou and Y. M. Cui, *China J. Chin. Mater. Med.*, 2018, **43**, 3498–3505.
34 Y. Q. Wang, L. Bao, D. L. Liu, X. L. Yang, S. F. Li, H. Gao, X. S. Yao, H. A. Wen and H. W. Liu, *Tetrahedron*, 2012, **68**, 3012–3018.
35 M. J. Frisch, G. W. Trucks, H. B. Schlegel, G. E. Scuseria, M. A. Robb, J. R. Cheeseman, G. Scalmani, V. Barone, B. Mennucci, G. A. Petersson, H. Nakatsuji, M. Caricato, X. Li, H. P. Hratchian, A. F. Izmaylov, J. Bloino, G. Zheng, J. L. Sonnenberg, M. Hada, M. Ehara, K. Toyota, R. Fukuda, J. Hasegawa, M. Ishida, T. Nakajima, Y. Honda, O. Kitao, H. Nakai, T. Vreven, J. A. Montgomery Jr, J. E. Peralta, F. Ogliaro, M. Bearpark, J. J. Heyd, E. Brothers, K. N. Kudin, V. N. Staroverov, R. Kobayashi, J. Normand, K. Raghavachari, A. Rendell, J. C. Burant, S. S. Iyengar, J. Tomasi, M. Cossi, N. Rega, J. M. Millam, M. Klene, J. E. Knox, J. B. Cross, V. Bakken, C. Adamo, J. Jaramillo, R. Gomperts, R. E. Stratmann, O. Yazyev, A. J. Austin, R. Cammi, C. Pomelli, J. W. Ochterski, R. L. Martin, K. Morokuma, V. G. Zakrzewski, G. A. Voth, P. Salvador, J. J. Dannenberg, S. Dapprich, A. D. Daniels, O. Farkas, J. B. Foresman, J. V. Ortiz, J. Cioslowski and D. J. Fox, *Gaussian 09, Revision A.02*, Inc., Wallingford, CT, 2009.